

# On the influence of statistics on the determination of the mean value of the depth of shower maximum for ultra high energy cosmic ray showers

**A. D. Supanitsky**

Instituto de Astronomía y Física del Espacio (IAFE), UBA-CONICET, Argentina.

E-mail: [supanitsky@iafe.uba.ar](mailto:supanitsky@iafe.uba.ar)

**G. Medina-Tanco**

Instituto de Ciencias Nucleares, UNAM, Circuito Exterior S/N, Ciudad Universitaria, México D. F. 04510, México.

E-mail: [gmtanco@nucleares.unam.mx](mailto:gmtanco@nucleares.unam.mx)

**Abstract.** The chemical composition of ultra high energy cosmic rays is still uncertain. The latest results obtained by the Pierre Auger Observatory and the HiRes Collaboration, concerning the measurement of the mean value and the fluctuations of the atmospheric depth at which the showers reach the maximum development,  $X_{max}$ , are inconsistent. From comparison with air shower simulations it can be seen that, while the Auger data may be interpreted as a gradual transition to heavy nuclei for energies larger than  $\sim 2-3 \times 10^{18}$  eV, the HiRes data are consistent with a composition dominated by protons. In Ref. [1] it is suggested that a possible explanation of the observed deviation of the mean value of  $X_{max}$  from the proton expectation, observed by Auger, could originate in a statistical bias arising from the approximated exponential shape of the  $X_{max}$  distribution, combined with the decrease of the number of events as a function of primary energy. In this paper we consider a better description of the  $X_{max}$  distribution and show that the possible bias in the Auger data is at least one order of magnitude smaller than the one obtained when assuming an exponential distribution. Therefore, we conclude that the deviation of the Auger data from the proton expectation is unlikely explained by such statistical effect.

## 1. Introduction

The nature of the primary cosmic rays is intimately related to the astrophysical objects capable of accelerating these particles to such high energies. Also, propagation in the intergalactic medium depends on the composition, which affects the resulting spectral distribution of the flux observed at Earth. A knowledge of the composition is also very important for primary energy reconstruction and for anisotropy studies.

One of the most important limitations of composition analyses comes from the lack of knowledge of the hadronic interactions at the highest energies. Composition studies are based on the comparison of experimental data with Monte Carlo simulations of atmospheric cosmic rays showers, which makes use of hadronic interaction models which extrapolate the available low energy accelerator data to the energies of the cosmic rays.

One of the most sensitive parameters to the mass of the primary cosmic ray is the atmospheric depth at which the showers reach their maximum development. Lighter primaries generate showers that are more penetrating, producing larger values of  $X_{max}$ . Also, the fluctuations of this parameter are smaller for heavier nuclei. The Pierre Auger Observatory and the HiRes experiment are able to observe directly the longitudinal development of the showers by means of fluorescence telescopes. Therefore, in both experiments, the  $X_{max}$  parameter of each observed shower can be reconstructed from the data taken by the telescopes.

The mean value and the standard deviation of  $X_{max}$ , as a function of primary energy, obtained by Auger [2] and HiRes [3] appear to be inconsistent. From the comparison with simulations, the Auger data suggest a transition to heavier nuclei starting at energies of order of  $2 - 3 \times 10^{18}$  eV, whereas, the HiRes data are consistent with protons in the same energy range. In Ref. [1] a new parameter, the difference between the mean value and the standard deviation of  $X_{max}$ , was introduced in order to reconcile the Auger and HiRes results. This new parameter has the advantage of being much less sensitive to the first interaction point than the mean value and the standard deviation separately. From a comparison of the experimental values of this parameter, obtained by Auger and HiRes, with simulated data, they infer that the composition of the cosmic rays is dominated by protons. They say that the energy dependence of the distribution of  $X_{max}$ , observed by Auger, seems to be caused by an unexpected change in the depth of the first interaction point, which can be explained by a rapid increase of the cross section and/or increase of the inelasticity. Both possibilities require an abrupt onset of new physics in this energy range, which makes them questionable. They also suggest that the deviation of the distribution of  $X_{max}$  from the proton expectation, present in the Auger data, could be originated in the statistical techniques used to analyze the data. In particular, they suggest that the deviation of the mean value of  $X_{max}$  from the proton expectation could be explained by a bias originated from the exponential nature of the  $X_{max}$  distribution and the decreasing number of events as a function of primary energy.

In this work we show that, considering a better description of the  $X_{max}$  distribution,

the bias in the determination of the mean value of  $X_{max}$  become more than one order of magnitude smaller than the one obtained for the exponential distribution. We find that the value of the bias in the last energy bin (the one with the smallest number of events) of the Auger data, published in Ref. [2], is  $\lesssim 1.5 \text{ g cm}^{-2}$ , which is much smaller than the systematic errors on the determination of the mean value of  $X_{max}$  estimated in Ref. [2].

## 2. Numerical approach

Following Ref. [1] let us introduce the parameter,

$$\xi(N) = 1 - \frac{\text{mode}[\bar{X}_{max}^N]}{\langle X_{max} \rangle}, \quad (1)$$

where  $\langle X_{max} \rangle$  is the mean value of the  $X_{max}$  distribution,

$$\bar{X}_{max}^N = \frac{1}{N} \sum_{i=1}^N X_{max}^i, \quad (2)$$

is the sample mean corresponding to samples of size  $N$  and  $\text{mode}[\bar{X}_{max}^N]$  is the value of  $\bar{X}_{max}^N$  that occurs most frequently, i.e. the maximum of the distribution function of  $\bar{X}_{max}^N$ . Therefore, the bias on the determination of  $\langle X_{max} \rangle$  appears when a particular realization of the sample mean is equal to the mode of the sample mean distribution function. Note that the sample mean (Eq. (2)) is an unbiased estimator of the mean of the exponential distribution, i.e.  $E[\bar{X}_{max}^N] = \langle X_{max} \rangle$ . In Ref. [1] it is shown that approximating the  $X_{max}$  distribution by an Exponential function the parameter  $\xi(N)$  is given by:  $\xi_E(N) = 1/N$ .

In order to better describe the distribution of  $X_{max}$  two different types of functions are considered. They are chosen in such a way that the distribution of  $\bar{X}_{max}^N$  can be obtained, at least, in a semi-analytical way. The first function considered is a shifted-Gamma distribution [4],

$$P_G(X_{max}) = \begin{cases} \frac{(X_{max} - X_0)^{k-1}}{\Gamma(k) \tau_X^k} \exp\left(-\frac{X_{max} - X_0}{\tau_X}\right) & X_{max} \geq X_0 \\ 0 & X_{max} < X_0 \end{cases}, \quad (3)$$

where  $k = 5$  and the other two parameters can be obtained from the mean value and the standard deviation of  $X_{max}$ ,

$$X_0 = \langle X_{max} \rangle - k \tau_X, \quad (4)$$

$$\tau_X = \frac{\sigma[X_{max}]}{\sqrt{k}}. \quad (5)$$

The second function under consideration is the convolution between an exponential function and a Gaussian (Exp-Gauss),

$$\begin{aligned} P_{EG}(X_{max}) &= \frac{1}{\lambda \sqrt{2\pi} \beta} \int_{-\infty}^{X_{max}} du \exp\left(-\frac{X_{max} - u}{\lambda}\right) \exp\left(-\frac{(u - \alpha)^2}{2\beta^2}\right) \\ &= \frac{1}{2\lambda} \exp\left(-\frac{X_{max} - \alpha}{\lambda} + \frac{\beta^2}{2\lambda^2}\right) \text{Erfc}\left(\frac{\beta}{\sqrt{2}\lambda} - \frac{X_{max} - \alpha}{\sqrt{2}\beta}\right), \end{aligned} \quad (6)$$

where  $\alpha$ ,  $\beta$  and  $\lambda$  are fitting parameters and

$$\text{Erfc}(z) = 1 - \frac{2}{\sqrt{\pi}} \int_0^z dt \exp(-t^2/2). \quad (7)$$

A library of simulated showers was generated by using the program CONEX (v2r2.3) [5]. Monochromatic samples of  $10^4$  proton showers were generated from  $\log(E/eV) = 18$  to  $\log(E/eV) = 19.5$  in steps of  $\Delta \log(E/eV) = 0.1$ . The arrival directions of the showers follow an isotropic distribution, such that the zenith angle is in the interval  $[0^\circ, 60^\circ]$ . The hadronic interaction models considered are QGSJET-II [6] and EPOS 1.99 [7].

The mean value and the standard deviation (needed for the description of the  $X_{max}$  distribution using the shifted-Gamma function) were fitted with a quadratic function and a linear function of  $\log(E)$ , respectively, i.e.,

$$\langle X_{max} \rangle = A_0 + A_1 \log(E/eV) + A_2 \log^2(E/eV), \quad (8)$$

$$\sigma[X_{max}] = B_0 + B_1 \log(E/eV). \quad (9)$$

Figure 1 shows the simulated data as well as the fits, for both hadronic interaction models considered. The values of the parameters corresponding to Eqs. (8) and (9) are

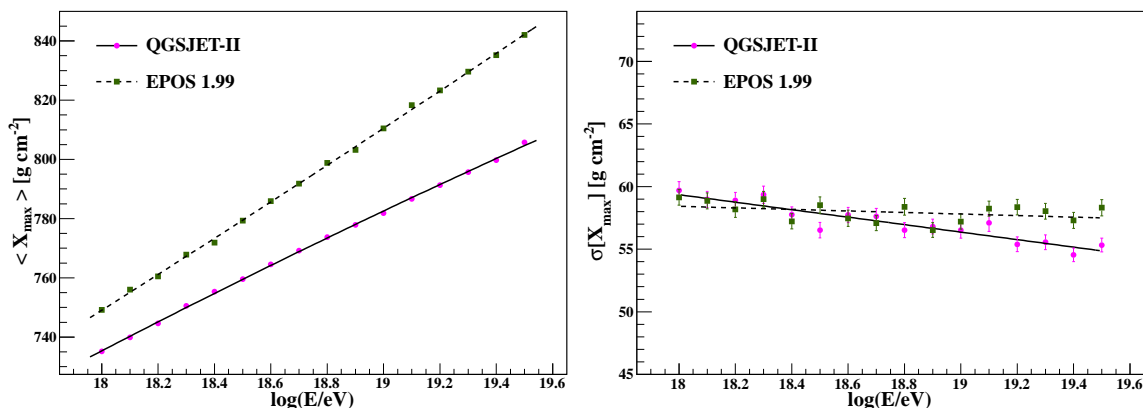


**Figure 1.** Mean value (left panel) and the standard deviation (right panel) of  $X_{max}$  as a function of  $\log(E/eV)$  obtained by using CONEX with QGSJET-II and EPOS 1.99 for proton initiated showers. The lines correspond to the fits of the simulated data (see the text for details).

given in table 1.

**Table 1.** Parameters corresponding to the quadratic and linear fits of  $\langle X_{max} \rangle$  and  $\sigma[X_{max}]$ , respectively (see Eqs. (8) and (9)), obtained from simulations for QGSJET-II and EPOS 1.99.

	$A_0$ [ $\text{g cm}^{-2}$ ]	$A_1$ [ $\text{g cm}^{-2}$ ]	$A_2$ [ $\text{g cm}^{-2}$ ]	$B_0$ [ $\text{g cm}^{-2}$ ]	$B_1$ [ $\text{g cm}^{-2}$ ]
QGSJET-II	-826.171	124.198	-2.08037	113.223	-2.99273
EPOS 1.99	80.4419	14.1183	1.27933	69.4862	-0.614616

The distribution functions of  $X_{max}$ , for every energy and hadronic interaction model considered, were fitted with the Exp-Gauss function, Eq. (6). The parameters  $\alpha$ ,  $\beta$  and  $\lambda$  were fitted with linear functions of  $\log(E)$ , in order to obtain the Exp-Gauss representation of the  $X_{max}$  distribution for every value of energy in the interval  $[10^{18}, 10^{19.5}]$  eV, see Appendix A for details.

Figure 2 shows the distributions of  $X_{max}$ , obtained by using CONEX with QJSJET-II, for  $\log(E/eV) = 19$  and  $\log(E/eV) = 19.5$ . Red solid lines correspond to the fits of the simulated data with the Exp-Gauss function. The blue dashed lines correspond to the shifted-Gamma function, Eq. (3), for which the parameters  $X_0$  and  $\tau_X$  are obtained by using the expressions of  $\langle X_{max} \rangle$  and  $\sigma[X_{max}]$  in Eqs. (8) and (9) to calculate  $X_0$  and  $\tau_X$  from Eqs. (4) and (5), respectively. From the figure it can be seen that the Exp-Gauss function is a better fit to the simulated data than the shifted-Gamma function. It can also be seen that the tail to larger values of  $X_{max}$  is slightly overestimated by the Exp-Gauss distribution and underestimated by the shifted-Gamma function. Therefore, the distribution function of the universe (samples with  $N \rightarrow \infty$ ) should fall between this two functions.

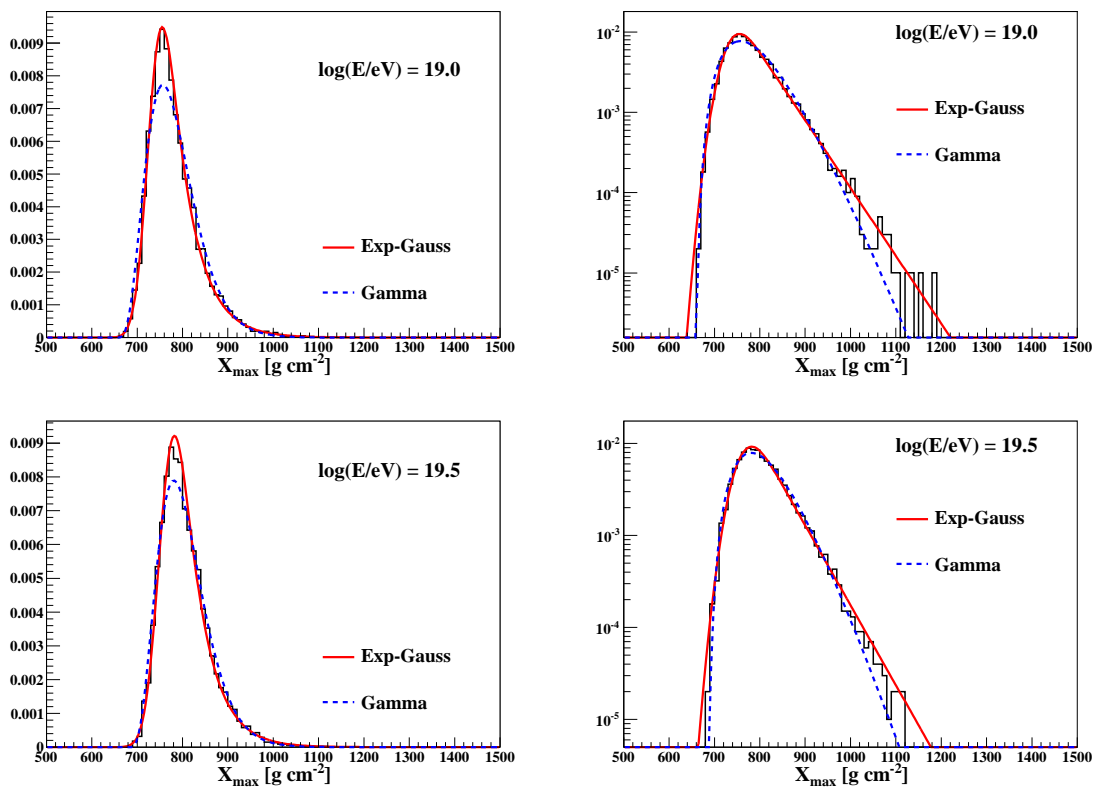


**Figure 2.** Distributions of  $X_{max}$  for proton showers generated by using CONEX with QJSJET-II. Red solid lines correspond to the fits of the histograms with the Exp-Gauss function, Eq. (6). The blue dashed lines correspond to the shifted-Gamma function, Eq. (3), where the parameters  $X_0$  and  $\tau_X$  are obtained by using Eqs. (4), (5), and the fits of  $\langle X_{max} \rangle$  and  $\sigma[X_{max}]$  as a function of  $\log E$  (see text for details).

The distribution of  $\bar{X}_{max}^N$  can be calculated by means of the characteristic function, which is defined as the expectation value of  $\exp(itX_{max})$ , i.e.  $\phi_{X_{max}}(t) = E[\exp(itX_{max})]$ . It is straightforward to show that the characteristic function of  $\bar{X}_{max}^N$  is given by  $\phi_{\bar{X}_{max}^N}(t) = [\phi_{X_{max}}(t/N)]^N$  [8].

The characteristic function of the shifted-Gamma distribution is  $\phi_{X_{max}}^G(t) = \exp(iX_0t) (1 - it\tau_X)^{-k}$  and then the characteristic function of  $\bar{X}_{max}^N$  is given by  $\phi_{\bar{X}_{max}^N}^G(t) = \exp(iX_0t) (1 - it\tau_X/N)^{-kN}$ , which corresponds also to a shifted-Gamma distribution. Therefore, the distribution function of  $\bar{X}_{max}^N$  is given by,

$$\bar{P}_G(\bar{X}_{max}^N) = \begin{cases} \frac{(\bar{X}_{max}^N - X_0)^{Nk-1}}{\Gamma(Nk) (\tau_X/N)^{Nk}} \exp\left(-\frac{\bar{X}_{max}^N - X_0}{\tau_X/N}\right) & \bar{X}_{max} \geq X_0 \\ 0 & \bar{X}_{max} < X_0 \end{cases} \quad (10)$$

By using Eq. (10) it is easy to show that,

$$\xi_G(N) = \frac{\sigma[X_{max}]}{\sqrt{k} \langle X_{max} \rangle} \frac{1}{N}. \quad (11)$$

In this case,  $\xi$  is also proportional to  $1/N$  but it is suppressed by the ratio between the standard deviation and the mean value of  $X_{max}$ . A similar expression is obtained when the distribution function of  $X_{max}$  is described by a truncated exponential function, see Appendix B for details. The blue solid line on the left panel of Fig. 3 corresponds to  $\xi_G$  as a function of  $N$  for  $\log(E/eV) = 19.5$ , approximately the mean value of the energy (weighted by the spectrum) for the last bin considered in Ref. [2]. Note that, the number of events in this bin is 34. From the figure, it can be seen that  $\xi_G$  is more than one order of magnitude smaller than the function  $1/N$ .

The distribution function of  $X_{max}$  is affected by the presence of fluctuations introduced by the detectors. The distribution function of  $\bar{X}_{max}^N$ , including a Gaussian uncertainty on the determination of  $X_{max}$  is given by,

$$\bar{P}_G^R(\bar{X}_{max}^N) = \frac{\sqrt{N}}{\sqrt{2\pi}\sigma_{Rec}} \int_0^\infty dX \bar{P}_G(X) \exp\left(-\frac{(\bar{X}_{max}^N - X)^2}{2\sigma_{Rec}^2/N}\right), \quad (12)$$

where  $\sigma_{Rec}$  is the standard deviation of such uncertainty. The mode of this distribution is calculated numerically. Dashed and dashed-dotted lines on the left panel of Fig. 3 correspond to parameter  $\xi_G(N)$  obtained for  $\sigma_{Rec} = 20 \text{ g cm}^{-2}$  and  $\sigma_{Rec} = 40 \text{ g cm}^{-2}$ , respectively. When a symmetric uncertainty on the determination of  $X_{max}$  is included, the parameter  $\xi$  becomes still smaller and decreases for increasing values of the uncertainty. This is due to the fact that  $\xi$  is larger for asymmetric distributions, like the exponential, and the convolution of the pure  $X_{max}$  distribution with a Gaussian is more symmetric than the original one.

The characteristic function of the Exp-Gauss distribution is the product of the characteristic function of the exponential distribution,  $(1 - i\lambda t)^{-1}$ , with the one corresponding to a Gaussian,  $\exp(i\alpha t - \beta^2 t^2/2)$ . Then, the characteristic function of  $\bar{X}_{max}^N$  is then given by,

$$\phi_{\bar{X}_{max}^N}^{EG}(t) = \left(1 - i\frac{\lambda}{N}t\right)^{-N} \exp\left(i\alpha t - \frac{\beta^2}{N}t^2/2\right), \quad (13)$$

which corresponds to the convolution of a Gamma distribution with a Gaussian,

$$\begin{aligned} \bar{P}_{EG}(\bar{X}_{max}^N) &= \frac{N^{N+1/2}}{\sqrt{2\pi}\beta\lambda^N\Gamma(N)} \int_{-\infty}^{\bar{X}_{max}^N} du (\bar{X}_{max}^N - u)^{N-1} \exp\left(-\frac{\bar{X}_{max}^N - u}{\lambda/N}\right) \\ &\quad \times \exp\left(-\frac{(u - \alpha)^2}{2\beta^2/N}\right). \end{aligned} \quad (14)$$

Last integral is calculated numerically in order to obtain the mode of the resultant distribution. The solid red line in the right panel of Fig. 3 shows  $\xi_{EG}$  as a function of the sample size for  $\log(E/eV) = 19.5$ . Note that  $\xi_G$  is smaller than  $\xi_{EG}$ , this is due to the more extended tail to larger values of the Exp-Gauss distribution compared with the corresponding one to the shifted-Gamma distribution. In any case,  $\xi_{EG}$  is still about one order of magnitude smaller than  $1/N$ . As for the case of the Gamma distribution, dashed and dashed-dotted red lines correspond to  $\sigma_{Rec} = 20 \text{ g cm}^{-2}$  and  $\sigma_{Rec} = 40 \text{ g cm}^{-2}$ , respectively. In this case the effect of the uncertainty on the determination of  $X_{max}$  is included in  $\bar{P}_{EG}$  just by replacing the parameter  $\beta$  by  $\tilde{\beta} = \sqrt{\beta^2 + \sigma_{Rec}^2}$ . As expected, the curves that include the uncertainty on the determination of  $X_{max}$  fall below the one corresponding to the ideal case.

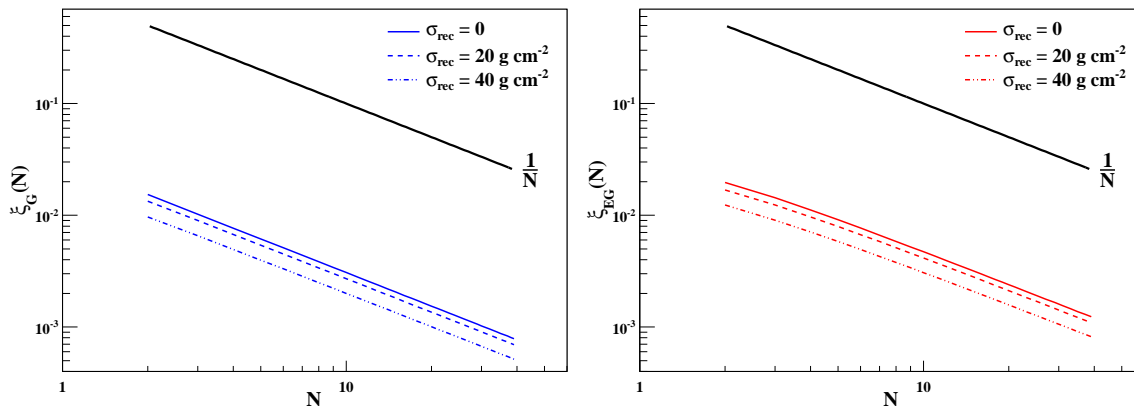


**Figure 3.**  $\xi$  as a function of the sample size  $N$  corresponding to proton showers of  $\log(E/eV) = 19.5$ , obtained for the shifted-Gamma distribution (left panel) and for the Exp-Gauss distribution (right panel). Blue and red solid lines correspond to the ideal case in which  $X_{max}$  is determined without any uncertainty. Dashed and dashed-dotted lines correspond to the cases in which there is a Gaussian uncertainty on the determination of  $X_{max}$  of  $\sigma_{Rec} = 20 \text{ g cm}^{-2}$  and  $\sigma_{Rec} = 40 \text{ g cm}^{-2}$ , respectively. The hadronic interaction model used is QGSJET-II.

The left panel of Fig. 4 shows the parameter  $\xi$  as a function of energy corresponding to the number of events in each energy bin taken from Ref. [2], for the case in which there is no uncertainty on the determination of  $X_{max}$  (which gives larger value of  $\xi$ , as shown before). The energy assigned to the  $i$ th bin, used to calculate  $\xi$ , corresponds to the mean value of the energy in the bin weighted by the broken power law fit of the

cosmic rays energy spectrum,  $J(E)$ , of Ref. [9],

$$\langle E_i \rangle = \frac{\int_{E_i^L}^{E_i^U} dE E J(E)}{\int_{E_i^L}^{E_i^U} dE J(E)}, \quad (15)$$

where  $E_i^L$  and  $E_i^U$  are the lower and upper limits of the  $i$ th bin. It can be seen that the values of  $\xi$ , obtained by using the Exp-Gauss distribution and the shifted-Gamma distribution, are more than one order of magnitude smaller than the corresponding one for the exponential distribution, in the whole energy range and for both hadronic interaction models considered. As in the previous calculation,  $\xi_G$  results are smaller than  $\xi_{EG}$ . In fact, the  $\xi$  curve corresponding to the true distribution of  $X_{max}$  should fall between the curves corresponding to the Exp-Gauss and the shifted-Gamma representation of the  $X_{max}$  distribution.

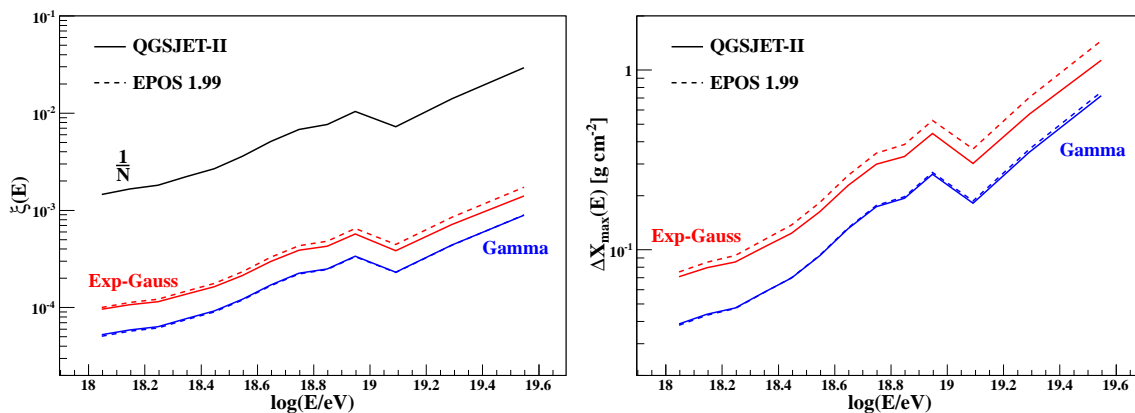


**Figure 4.**  $\xi$  (left panel) and  $\Delta X_{max}$  (right panel) as a function of  $\log(E/eV)$ , for the statistics of the Auger data of Ref. [2]. Solid lines correspond to QGSJET-II and dashed lines correspond EPOS 1.99.

The right panel of Fig. 4 shows the parameter  $\Delta X_{max} = \langle X_{max} \rangle \xi$  which gives the grammage of the shift suffered by  $\langle X_{max} \rangle$  if  $\bar{X}_{max}^N$  takes the value of the mode of its distribution. It can be seen, that for the last energy bin, the one with 34 events,  $\Delta X_{max}$  is  $\lesssim 1.5 \text{ g cm}^{-2}$ , which is much smaller than the systematic uncertainties on the determination of  $\langle X_{max} \rangle$  estimated in Ref. [2].

The energy bins considered in the analysis of Ref. [2] have a width of  $\Delta \log(E/eV) = 0.1$  in the energy range from  $E = 10^{18} \text{ eV}$  to  $E = 10^{19} \text{ eV}$ . Between  $E = 10^{19} \text{ eV}$  and  $E = 10^{19.4} \text{ eV}$ ,  $\Delta \log(E/eV)$  changes to 0.2 and the last bin corresponds to  $E \geq 10^{19.4} \text{ eV}$ . Therefore, the number of events per bin decreases in the energy range from  $E = 10^{18} \text{ eV}$  to  $E = 10^{19} \text{ eV}$ , it increases from 96 in the bin  $[10^{18.9}, 10^{19}] \text{ eV}$  to 138 in the bin  $[10^{19}, 10^{19.2}] \text{ eV}$  and then, it decreases for the last two bins. This change in the bin width generates the structure around  $E \cong 10^{19.1} \text{ eV}$  seen on the curves of Fig. 4.

Note that  $\xi_{EG}$  calculated by using EPOS 1.99 is larger than the corresponding one for QGSJET-II, this is due to the fact that the  $X_{max}$  distributions obtained with EPOS



1.99 are more asymmetric (increase faster, coming from small values of  $X_{max}$ , and have a more extended tail) than the corresponding ones to QGSJET-II.

Concerning iron showers, it can be seen that  $\xi$  takes smaller values than the ones for protons. This is due to the large suppression of fluctuations in iron showers, the ratio of the standard deviation to the mean value of  $X_{max}$  is smaller than for protons, producing smaller values of  $\xi$  (see Eq. (11)). In particular,  $\xi_G^{fe} = \xi_G^{pr}/K$  where  $K$  increases from  $\sim 2.3$  at  $E = 10^{18}$  eV to  $\sim 2.4$  at  $E = 10^{19.5}$  eV for QGSJET-II.

### 3. Conclusions

In this work we studied in detail statistical bias in the determination of the mean value of  $X_{max}$ , suggested in Ref. [1], as a possible explanation of the deviation of Auger data from the proton expectation. We used two different functions to fit the  $X_{max}$  distribution obtained from simulations: (i) the convolution of an Exponential distribution with a Gaussian and (ii) a shifted-Gamma distribution. We find that the bias obtained by using these two functions is more than one order of magnitude smaller than the corresponding one of the Exponential distribution, the one used in Ref. [1]. We find that the values of the bias, obtained for the convolution of the Exponential function with the Gaussian, are larger because it presents a more extended tail to larger values of  $X_{max}$  than the shifted-Gamma distribution. We also find that the bias diminishes when a Gaussian (symmetric) uncertainty on the determination of  $X_{max}$  is included.

We also calculated the expected bias, as a function of primary energy, using the actual number of events in each energy bin of the Auger data, published in Ref. [2], for both hadronic interaction models considered in this work, QGSJET-II and EPOS 1.99. We find that the largest value of the bias, corresponding to the bin with the smallest number of events, is smaller than  $1.5 \text{ g cm}^{-2}$ , much less than the systematic errors on the determination of  $\langle X_{max} \rangle$  estimated in Ref. [2].

### Appendix A. Parameters for the Exp-Gauss fits

The parameters  $\alpha$ ,  $\beta$  and  $\lambda$ , obtained from the fits of the  $X_{max}$  distributions with the Exp-Gauss function (see Eq. (6)), are fitted with linear functions of  $\log(E/eV)$  as shown in figure A1. They can be written in the following way,

$$\begin{pmatrix} \alpha(E) \\ \beta(E) \\ \lambda(E) \end{pmatrix} = \begin{pmatrix} C_1 & C_2 \\ C_3 & C_4 \\ C_5 & C_6 \end{pmatrix} \begin{pmatrix} 1 \\ \log(E/eV) \end{pmatrix}, \quad (\text{A.1})$$

where the coefficients  $C_i$ ,  $i = 1..6$ , are given in table A1 for both hadronic interaction models considered.

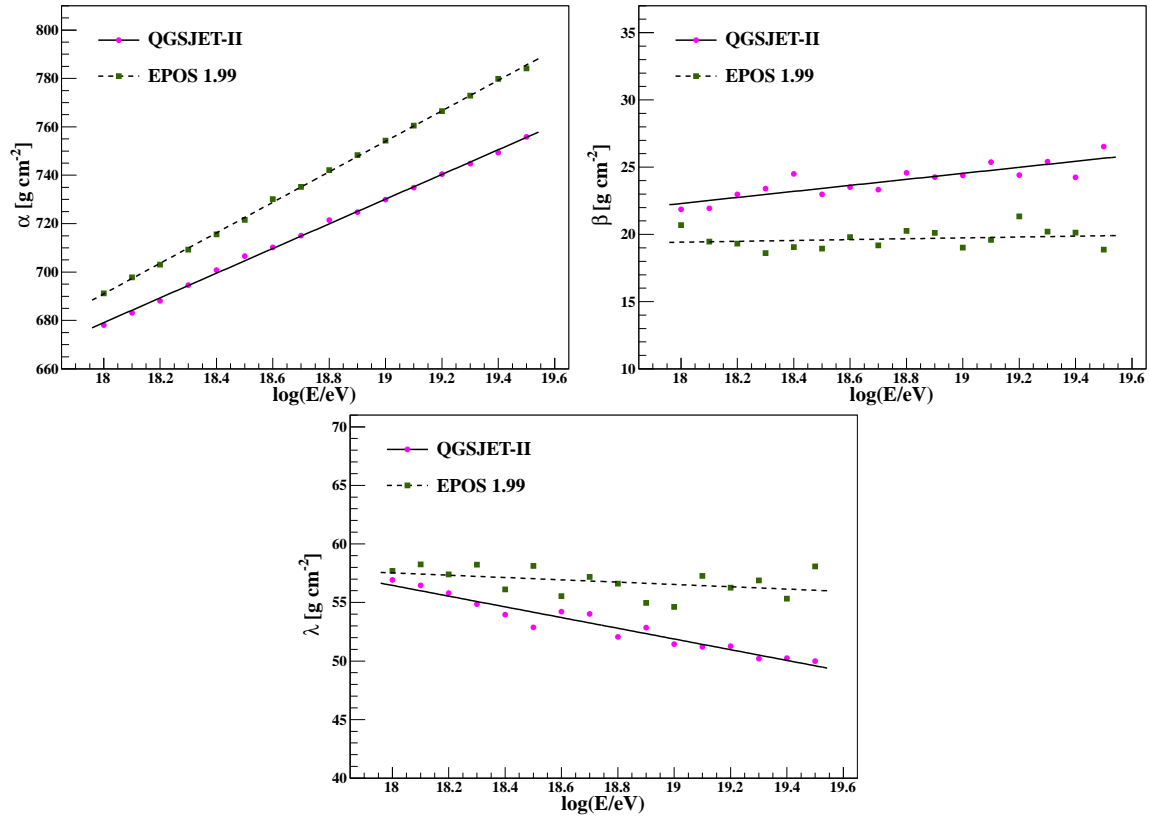


**Figure A1.** Parameters  $\alpha$ ,  $\beta$  and  $\lambda$  corresponding to the fits of the  $X_{max}$  distribution with the Exp-Gauss function for QGSJET-II and EPOS 1.99. The straight lines correspond to the linear fits of the points.

**Table A1.** Coefficients  $C_i$ , in  $[g\text{ cm}^{-2}]$ , corresponding to QGSJET-II and EPOS 1.99.

	$C_1$	$C_2$	$C_3$	$C_4$	$C_5$	$C_6$
QGSJET-II	-239.053	51.0096	-18.0164	2.23981	138.806	-4.57508
EPOS 1.99	-443.120	63.0078	13.6458	0.320823	75.2960	-0.987241

## Appendix B. Calculation of $\xi$ for a truncated exponential distribution

It is possible to describe the  $X_{max}$  distribution function by a truncated exponential distribution, which is given by,

$$P_{TE}(X_{max}) = \begin{cases} \frac{1}{\Lambda} \exp\left(-\frac{X_{max} - X_c}{\Lambda}\right) & X_{max} \geq X_c \\ 0 & X_{max} < X_c \end{cases}, \quad (\text{B.1})$$

where  $\Lambda$  is a parameter that describe the tail of the  $X_{max}$  distribution and  $X_c$  is the truncation value.

The characteristic function of this distribution is,  $\phi_{X_{max}}^{TE}(t) = \exp(itX_c) (1 - it\Lambda)^{-1}$  and then, the characteristic function of the sample mean is given by,  $\phi_{\bar{X}_{max}}^{TE}(t) =$

$\exp(itX_c) (1 - it\Lambda/N)^{-N}$ , which corresponds to a shifted Gamma distribution. Therefore, the distribution function of the sample mean is given by,

$$\bar{P}_{TE}(\bar{X}_{max}^N) = \begin{cases} \frac{(\bar{X}_{max}^N - X_c)^{N-1}}{\Gamma(N)(\Lambda/N)^N} \exp\left(-\frac{X_{max} - X_c}{\Lambda/N}\right) & \bar{X}_{max}^N \geq X_c \\ 0 & \bar{X}_{max}^N < X_c \end{cases}. \quad (\text{B.2})$$

By using that  $\langle X_{max} \rangle = X_c + \Lambda$ , it is easy to show that,

$$\xi_{TE}(N) = \frac{\Lambda}{\Lambda + X_c} \frac{1}{N}, \quad (\text{B.3})$$

$$= \frac{\sigma[X_{max}]}{\langle X_{max} \rangle} \frac{1}{N}. \quad (\text{B.4})$$

Note that, it can be seen, from Eq. (B.4), that  $\xi_{TE}$  takes a very similar form to the one obtained for the shifted-Gamma function, see Eq. (11).

Typical values of the parameters, obtained experimentally, are  $X_c \cong 700 \text{ g cm}^{-2}$  and  $\Lambda \cong 56 \text{ g cm}^{-2}$  [10] (note that these parameters depend on primary energy and the ones used here, obtained from Ref. [10], correspond to the energy interval  $[10^{18}, 10^{18.5}]$  eV, in any case, they are just used to roughly estimate the suppression factor of the bias). Therefore,  $\xi_{TE}(N) \cong 0.125/N$ , which is suppressed by a factor 0.125 with respect to the corresponding one to the exponential distribution.

## References

- [1] G. Wilk and Z. Wlodarczyk 2011 *J. Phys. G:Nucl. Part. Phys.* **38** 085201.
- [2] J. Abraham et al. 2010 *Phys. Rev. Lett.* **104** 091101.
- [3] R. Abbasi et al. 2010 *Phys. Rev. Lett.* **104** 161101.
- [4] F. Schmidt, M. Ave, L. Cazon, and A. Chou 2008 *Astropart. Phys.* **29** 355.
- [5] T. Bergmann et al. 2007 *Astropart. Phys.* **26** 420.
- [6] S. Ostapchenko 2006 *Nucl. Phys. Proc. Suppl.* **B 151** 143.
- [7] T. Pierog and K. Werner 2006 *Phys. Rev. Lett.* **101** 171101.
- [8] F. James 2006 *Statistical Methods in Experimental Physics* World Scientific Publishing.
- [9] J. Abraham et al. 2010 *Phys. Lett.* **B 685** 239.
- [10] R. Ulrich for the Pierre Auger Collaboration 2011 *Proceedings of 32nd ICRC, Beijing* **5** 51 (arXiv:1107.4804).